15th International Symposium on Computer Methods in Biomechanics and Biomedical Engineering
and
3rd Conference on Imaging and Visualization
CMBBE 2018
P. R. Fernandes and J. M. Tavares (Editors)

Numerical simulation of the deployment process of a new stent produced by ultrasound-microcasting: the role of the balloon's constitutive modeling

I.V. Gomes*, H. Puga*, J.L. Alves*

*CMEMS – Center for Microelectromechanical Systems
Department of Mechanical Engineering, University of Minho, Campus of Azurém, 4800-058 Guimarães, Portugal
b7405@dem.uminho.pt
puga@dem.uminho.pt
jlalves@dem.uminho.pt

Keywords: Stent Deployment, Material Constitutive Modeling, Finite Element Analysis.

Abstract: *The application of the finite element method (FEM) allows to predict the behavior of a stent during the deployment process and when in service, being a powerful tool to use in its design and development.*

As the promoter of the stent expansion, the balloon plays a very important role, offering a strong influence on its performance, mainly during the deployment process. This element is usually built in a rubber-like material such as polyurethane, being modelled as linear elastic or hyperelastic with a Mooney-Rivlin description.

This work aims, through FEM analysis, the study of the influence of both adopted material formulation – linear elastic or hyperelastic -, as well as the respective material constants and properties for the balloon modeling and its geometry on the performance of a biocompatible magnesium stent regarding a set of metrics. Furthermore, a comparison is established between those results and the obtained ones in the scenario of application of pressure directly in the inner surface of the stent, neglecting the balloon.

The obtained results suggest that material formulation has direct influence on the stent deployment process. Concerning to hyperelastic models, three different combinations of parameter values were tested, showing a similar behavior in terms of dogboning and foreshortening, while the required expansion pressure was significantly different. The same relation was found between the results obtained with the tested linear elastic models, while the scenario of neglecting the balloon suggests providing the highest values of dogboning, foreshortening and recoil, with an expansion pressure comparable to that of hyperelastic models.

1 INTRODUCTION

Coronary heart disease such as atherosclerosis is, nowadays, one of the major causes of death in the world [1]. One of the possible treatments for this condition is the deployment of a stent, a tiny wire mesh tube-like structure, which is radially expanded through the inflation

of a balloon placed within it, reopening the vessel and acting as a scaffold [2, 3].

The Finite Element Method (FEM) is a powerful tool used in the study, design, and development of these devices, once it allows to predict their behavior in a more expeditious way with lower costs when compared to the experimental techniques [4]. Thus, to guarantee that the obtained results are trustworthy, it is crucial the correct definition of the system, namely in terms of the material constitutive models applied to the involved constituents, including the stent and the balloon.

As the promoter of the stent expansion, the balloon plays a very important role, having a strong influence on its performance, mainly during the deployment process. This element is made of rubber-like materials such as polyurethane [4-7] or nylon [8] and its constitutive behavior is modelled through different formulations, being the most commons the linear elastic and the hyperelastic with Mooney-Rivlin description. Such definition is suggested to have impact on the results obtained by the analysis by FEM and, therefore, on their applicability to the reality. Besides some authors such as Wang *et al.* [9], Gervaso *et al.* [10] and Pant *et al.* [11] have adopted the linear elastic model for cylindrical-shaped balloons, this formulation is more common when a folded balloon geometry is used as presented by Schiavone *et al.* [5, 12, 13] and De Beule *et al.* [6]. Indeed, the rubber-like materials are characterized by its incompressibility or near-incompressibility and highly nonlinear behavior at large strains; however, in the region of small strains, which is characterized by a linear behavior, a Young's modulus may be assigned [14]. Hyperelastic models with Mooney-Rivlin description were preferred for cylindrical balloons modeling by Chua *et al.* [15], Schiavone *et al.* [5], Eshghi *et al.* [7] and Beigzadeha *et al.* [16] with different values for material parameters. The material constants are derived from experimental data of mechanical tests, the reason why different tests may lead to different values. Consequently, the mechanical tests to perform to provide information for the material constants calculation must represent a stress state as close as possible to the one that the studied element expectedly undergoes to describe the material behavior in a reliable way. The aforementioned relation between geometry and material constitutive modeling and its impact on the trustworthiness of the results obtained by Finite Element Analysis (FEA) highlights these two factors as of major importance and, therefore, as deserving a study focused on it.

Hence, the present work aims the study by FEM of the influence of the adopted material formulation – linear elastic or hyperelastic - and respective material constants and properties for the balloon modeling on the performance of a biocompatible magnesium alloy stent. Furthermore, a comparison is established between those results and the obtained ones in the scenario of application of pressure directly in the inner surface of the stent to mimic the presence of the balloon.

2 DESCRIPTION OF THE METHODOLOGY

In the present work, the influence of balloon material constitutive modeling is assessed through the use of two different material formulations – linear elastic, with two different values of Young's modulus, referred as Linear Elastic 1 (LE1) and Linear Elastic 2 (LE2), and hyperelastic with Mooney-Rivlin description, being used three different set of material parameters, designated as Hyperelastic 1 (HE1), Hyperelastic 2 (HE2) and Hyperelastic 3 (HE3).

A simpler simulation is performed neglecting the presence of the balloon. In this case, the stent expansion is promoted by the application of a linear pressure directly in the inner surface of the stent until the target diameter is reached, after what the stent slightly recoils by

the absence of applied load, what mimics the deflation of the balloon.

When considering the inflation of the balloon within the stent, a linear pressure is applied on its inner surface, leading to its expansion and, consequently, to the radial deformation of the stent. An augmented Lagrange formulation is adopted for the contact between the stent and the balloon, which is considered frictionless. This method allows to produce less penetration and better accuracy than the pure penalty method presenting, however, higher computational cost.

2.1 Geometry

The NG stent geometry [17] results of a combination of straight lines and arcs, which are expected to contribute to both reduction of the expansion pressure and foreshortening phenomenon. The linkage between the rings of the structure is made using curved "bridge" elements, whose deformation during the expansion process allows the compensation of the length reduction due to the radial expansion. The nonexpanded inner diameter of the stent and its length is 5 mm and 24 mm, respectively, and its thickness is equal to 0.1 mm.

This geometry presents periodicity in the circumferential and longitudinal directions in the cylindrical coordinate system as it is formed by the assembling of multiple identical unit cells. Along with the geometrical periodicity, the isotropic behavior of the material allows the use of only one-tenth (1/5 in the circumferential direction and 1/2 in the longitudinal direction) of the model, reducing the required computation time thanks to a smaller number of degrees of freedom (DOFs) while the accuracy of the results is guaranteed. For this purpose, symmetry conditions are applied to all degrees of freedom of the stent belonging to planar faces α, β and γ, as shown in Figure 1(a).

A cylindrical balloon with open ends is used to promote the radial expansion of the stent, presenting an inner diameter equal to 4.7 mm, thickness of 0.15 mm and a full length of 26 mm. Once again, due to the geometrical symmetry and isotropic behavior of the material, only one-tenth of the balloon model is used, being applied symmetry conditions on all the degrees of freedom that belong to the planar faces α, β and γ, as presented in Figure 1(a), being the ends fully constrained to represent the bond to the catheter. The assembly of both elements (stent and balloon) is presented in Figure 1(b).

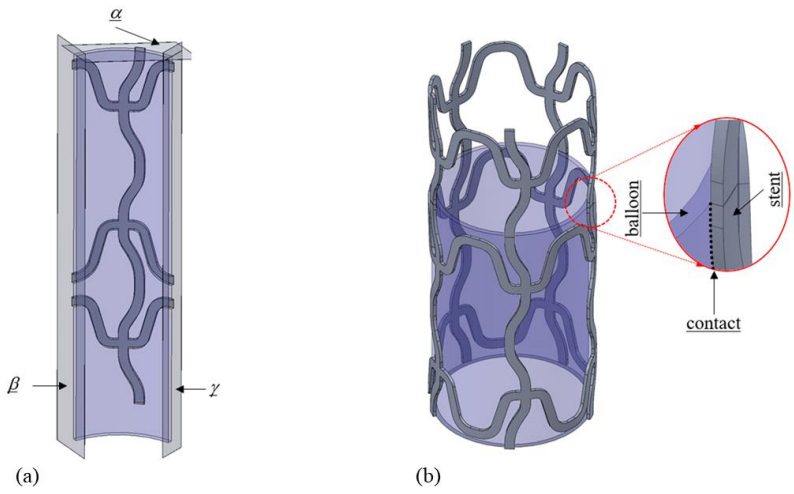

Figure 1 Balloon and stent set (a) identification of the planes of symmetry; (b) assembly of balloon and stent with identification of the contact area

2.2 Material Constitutive Modeling

The material selected for the stent is a magnesium alloy whose mechanical behavior, due to the manufacturing process, is assumed to be isotropic and elastoplastic with Young's modulus $E = 43\ GPa$ and Poisson ratio $v = 0.30$, being the plastic behavior modelled by the von Mises yield criterion. The nonlinear isotropic stress-strain hardening curve is modelled by a Voce-type law defined by Equation (1).

$$\sigma = \sigma_0 + (\sigma_{sat} - \sigma_0)(1 - \exp(-C_y \times \bar{\varepsilon}^p)) \tag{1}$$

where σ_0 is the initial yield stress, equal to 174.8 MPa, σ_{sat} is the saturation flow stress, equal to 315.6 MPa, C_y is the unitless hardening rate, equal to 16.3 and $\bar{\varepsilon}^p$ is the equivalent plastic strain, work-conjugate of the von Mises equivalent stress.

The constitutive modeling of balloon hyperelastic material, characterized by low elastic modulus and high bulk modulus, is derived from the strain energy function (W), which represents the energy stored in the material per unit of reference volume, based on three strain invariants of the Cauchy-Green deformation tensor ($\bar{I}_1$, $\bar{I}_2$ and $\bar{I}_3$). Once hyperelastic materials are considered incompressible, $\bar{I}_3$ is equal to 1 and W becomes a function dependent only on $\bar{I}_1$ and $\bar{I}_2$.

One of the possible formulations for the description of the behavior of hyperelastic materials are Mooney-Rivlin models, whose generic expression is given by Equation (2):

$$W = \sum_i \sum_j C_{ij} (\bar{I}_1 - 3)^i (\bar{I}_2 - 3)^j + \frac{1}{D_1} (J_{el} - 1)^2 \tag{2}$$

where $\bar{I}_1$ and $\bar{I}_2$ are the first and second invariant of the left isochoric Cauchy-Green deformation tensor, J_{el} is the elastic Jacobian and C_{ij} and D_1 are model parameters, resulting from materials experimental data from mechanical tests.

In this study, a two-parameter Mooney-Rivlin model is used to describe the behavior of polyurethane rubber, according to Equation (3), being tested the values of the material constants presented in Table 1.

$$W = C_{10} (\bar{I}_1 - 3) + C_{01} (\bar{I}_2 - 3) + \frac{1}{D_1} (J_{el} - 1)^2 \tag{3}$$

Material Model	C_{10} **[MPa]**	C_{01} **[MPa]**	D_1 **[-]**
HE1	1.03 [5]	3.69 [5]	0 [5]
HE2	1.07 [15, 18]	0.71 [15, 18]	
HE3	-0.89	5.39	

Table 1: Material constants for hyperplastic material models.

The values of the material constants of HE3 model were obtained through curve fitting of experimental data from a uniaxial tensile test performed on a polyurethane sample.

Regarding the linear elastic behavior modeling of balloon material, two different values of Young's modulus were studied, being considered the same value of Poisson ratio for both

situations, as presented in Table 2.

Material Model	E **[MPa]**	ν **[-]**	ρ **[Kg/m3]**
LE1	10 [9]	0.49 [9]	1100 [6]
LE2	920 [6, 11]		

Table 2: Elastic properties of linear elastic material models.

4 RESULTS AND DISCUSSION

Figure 2 presents the required expansion pressure as function of the expanded radius of the stent. The analysis of the results suggests that the adoption of LE2 model provides significantly higher values of expansion pressure (more than 50 times superior) than those of the remaining models to promote the same radial deformation of the stent. The deformation of the balloon belongs to large strains domain and it is noticeable the impact of the adopted value of Young's modulus in the obtained results. Indeed, it may be suggested that the use of a value as high as that of LE2 model for a cylindrical balloon may not be a suitable option to describe the real behavior of the rubber-like material, once it is expected a softer slope with a smooth and gradual increase of the stress with a more significant increase of the strain, which reaches values superior to 100%. However, the elastic properties of LE2 model are, possibly, appropriated for the modeling of a folded balloon, as secondary mechanisms such as self-contact are involved in the expansion of the balloon and additional resistance is expected until the unfolding be completed, i.e., in the first stage of pressure application, the balloon will not experience a significant radial deformation as it presents overlapping sections.

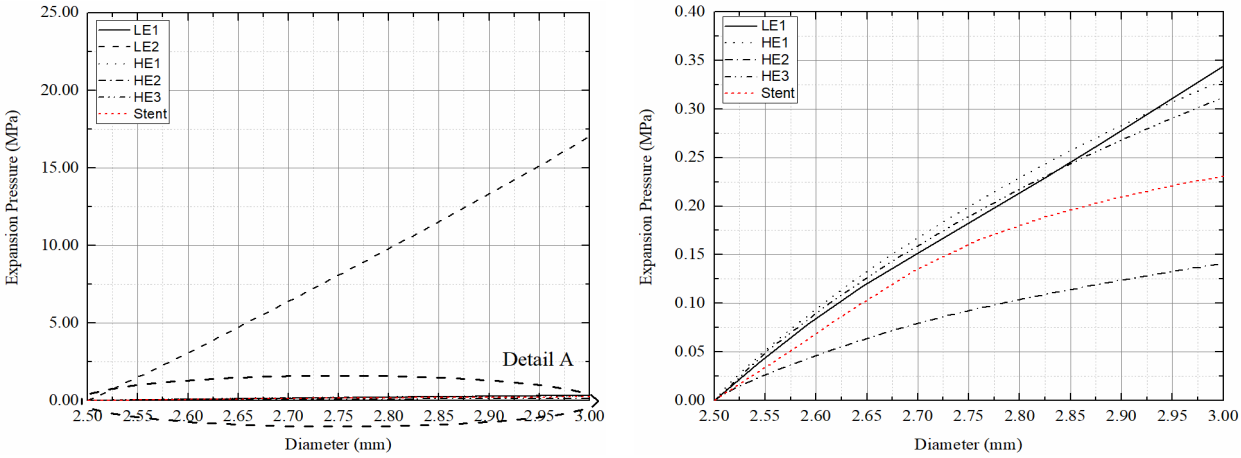

Figure 2: (a) Required expansion pressure as function of the expanded radius of the stent; (b) Detail A.

The use of LE1 model shows results close to those obtained through the adoption of HE1 and HE3 models, being the difference equal to approximately 2.94% (0.34 MPa vs 0.33 MPa) for the first and 8.82% for the second. Concerning to HE2 model, it presents significantly lower values of expansion pressure (0.14 MPa), about 58.82% inferior to LE1 results, for the same expanded diameter of the stent. These results also highlight the influence of the material parameters used in the Mooney-Rivlin description in the behavior of the material, reinforcing the importance of the adequate selection of the mechanical tests to perform to trustworthly characterize it. According to the aforesaid, it is suggested that the adoption of a linear elastic approach to the constitutive modeling of a hyperelastic material for a cylindrical

balloon may be a valid option as a similar behavior was found between the LE1, HE1 and HE3 models.

The simulation of the stent itself leads to values of required expansion pressure comparable to those of HE1, HE3 and LE1 models, being superior to the presented ones by HE2 model, supporting that such simplification may provide adequate results with minor computational cost.

Another studied performance parameter was dogboning, being its evolution as function of the expansion pressure shown in Figure 3.

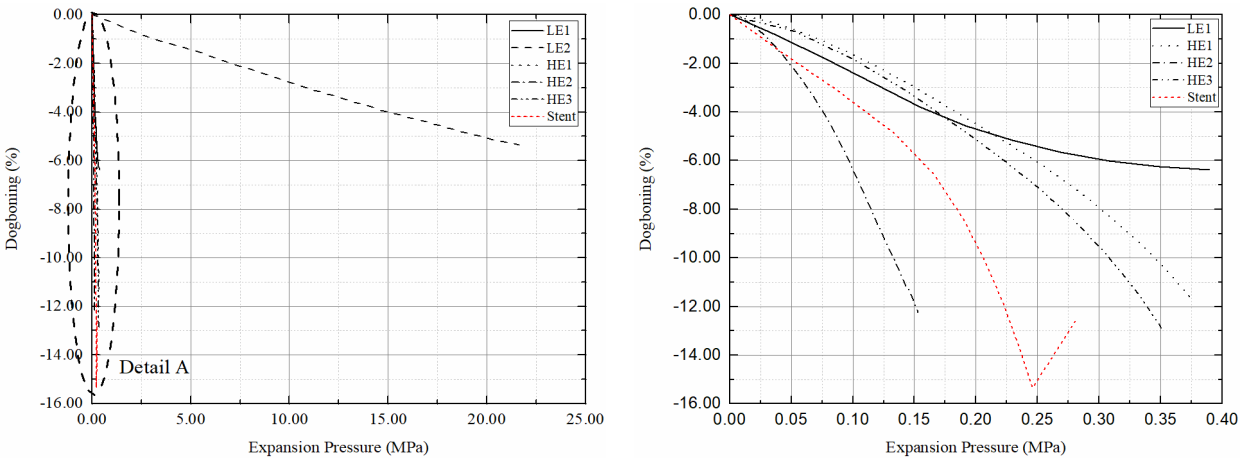

Figure 3: (a) Evolution of dogboning parameter as function of the expansion pressure (b) Detail A.

All the studied cases present negative values of dogboning, which means that the central region of the stent experiences greater expansion than its ends. All the models present an increase of dogboning as the expansion pressure rises excepting the direct pressurization of the stent, being the hyperelastic models (HE1, HE2 and HE3) the ones that present higher values with post-dilatation absolute values of 11.60%, 12.23% and 13.02%, respectively. The difference between LE2, the lowest value, and HE1 models is about 53.94%. When the presence of the balloon is neglected, the dogboning effect presents a different behavior comparing to that of other scenarios, as its maximum value is not reached at full expansion. Once the application of the pressure is ceased as the target diameter is reached in each point, the recoil phenomenon does not occur simultaneously for all the structure, resulting in that the central section of the stent experiences it first than its ends. This situation leads to the presented inversion of the dogboning tendency. This scenario is also associated with the greatest value of dogboning (-12.61%), which is possibly explained by the inexistence of a physical barrier that prevents the sudden recovery of the elastic deformation of the structure, as it happens when the balloon is considered. Conversely to what is verified for the relation between the applied expansion pressure and the stent's diameter, the dogboning effect suggests being more sensitive to the adoption of a linear model instead of a hyperelastic one, as well as to the neglection of the balloon, as more relevant discrepancies are found between the results presented by these models.

The results obtained in foreshortening evaluation are presented in Figure 4 and show that the adoption of hyperelastic formulations for modeling the constitutive behavior of balloon leads to an elongation (positive values of foreshortening) of the stent in the initial phase of the expansion that evolves then to its shortening (negative values of foreshortening), in agreement with the remaining models. Along with the fact that both linear elastic models

(LE1 and LE2) present significantly higher values of foreshortening when compared to those of hyperelastic ones, it is once again highlighted the influence of the adopted material formulation in the behavior of the system. As verified for dogboning, when a pressure is applied directly in the inner surface of the stent, the maximum absolute value of foreshortening (-0.53%) does not occur at its maximum diameter, which may have origin on the aforementioned mechanism.

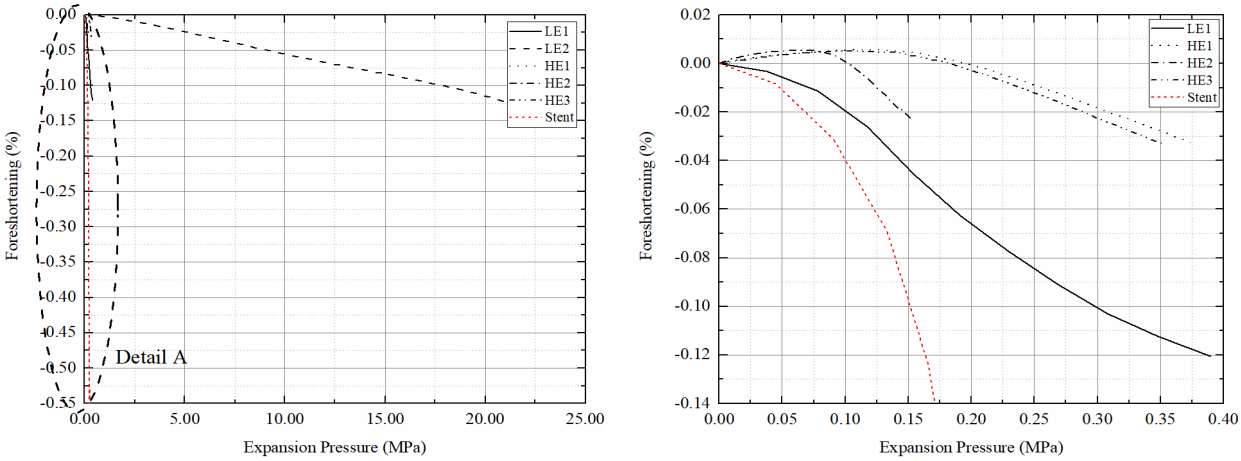

Figure 4: (a) Evolution of foreshortening parameter as function of the expansion pressure (b) Detail A.

The different behavior presented by the linear elastic and hyperelastic models and between each set of material properties (Young's modulus) and parameters (Mooney-Rivlin constants) may also be promoted by the contact formulation between the stent and the balloon, as there are related variables strongly dependent on them. Indeed, the characteristic stiffness of the contact is dependent on the equivalent Young's modulus, whose value is equal to the Young's modulus itself in the case of linear elastic models, but that depends on the bulk modulus and on the Mooney-Rivlin constants for hyperelastic formulations, giving origin to different values.

After the complete expansion of the stent promoted by the balloon inflation, the ballon is deflated in order to be extracted along with the further elements used in the deployment process. At this stage, the pressure exerted by the balloon in the inner surface of the stent ceases and the elastic portion of its deformation is recovered causing a phenomenon called recoil, which can be longitudinal, central and distal. The obtained values for these metrics are presented in Table 3.

	Longitudinal Recoil (%)	**Distal Recoil (%)**	**Central Recoil (%)**
LE1	-0.08	2.98	6.22
LE2	-0.07	1.96	4.27
HE1	0.002	2.95	7.12
HE2	0.006	3.47	9.28
HE3	0.003	2.86	7.33
Stent	-0.36	5.58	9.27

Table 3: Recoil evaluation.

Concerning to the longitudinal recoil, which corresponds to the variation of the stent's length as the balloon is deflated, all the studied cases with exception of the hyperelastic models show negative values and, therefore, a shrinkage of the device. The values of longitudinal recoil presented by HE1, HE2 and HE3 models are significantly inferior to those of the remaining scenarios and close to zero, meaning that there is no relevant alteration of the length of the stent due to its elastic recovery. The obtained values for the linear elastic models LE1 and LE2 are similar, while the simulation of the stent without balloon leads to the highest absolute value (-0.36%).

The distal recoil corresponds to the difference between the stent's diameter in its ends in the fully expanded configuration and after the balloon deflation. Regarding this parameter, it is noticeable that the LE1, HE1 and HE3 models present comparable values, whilst the lowest value is that of LE2 model (1.96%) and the highest one is the obtained through the neglection of the balloon (5.58%). Indeed, the LE1 value is only about 1.02% superior to that of HE1, while this difference is about 46.59% compared to the use of the stent itself and approximately equal to 50.51% relatively to LE2 model.

The difference between the stent's diameter in its mid-region in the aforementioned conditions is called central recoil. The obtained results show that this phenomenon is more relevant than the distal recoil, once higher values are achieved, existing a greater reduction of the stent's expanded diameter in the central part. Regarding this parameter, the values presented by the stent itself (9.27%) and the HE2 model (9.28%) are the highest ones, being significantly above those presented by the other models.

The occurrence of such phenomena is a situation with negative impact on the performance of the stent once it may demand an overexpansion of the device in order to take into consideration its diameter loss after the deflation of the balloon, which can compromise the integrity of the blood vessel and, therefore, the success of the procedure.

5 CONCLUSIONS

In the present work, a systematic study of the influence of the adopted material formulation for the expansion balloon modeling was performed. The main conclusions to be drawn from this study are:

(1) the choice of the material constitutive model of the expansion balloon suggests having a significant influence on the stent deployment process simulation.

(2) the adoption of different material formulations leads to different results of the considered performance metrics, possibly driving to significant discrepancies between the results obtained through numerical analysis and those then presented by the device in real context. Such situation may have as consequence the inadequacy of the numerical model to correctly describe the behavior of the system, not providing results close to reality and, therefore, invalidating the stent's designs proposed by it.

(3) the adoption of a linear elastic model may be suitable for the description of the relation between expansion pressure and expanded radius for a cylindrical balloon built in a rubber-like material if a low Young's modulus is assigned. Concerning to the evaluation of the remaining performance metrics, this option does not suggest being a so-appropriate approach, as more significant differences relatively to hyperelastic models are noticed (about 45.17% for dogboning and 26.97% for foreshortening relatively to HE1 model).

(4) the use of high values of Young's modulus as that of LE2 model appears not to fit the description of the cylindrical-shaped balloon behavior, mainly in terms of the process

of radial deformation of the stent, being suggested that it is required an expansion pressure more than fifty times superior to that demanded by the other models. This option is possibly suitable for the modeling of a folded balloon.

(5) The direct application of pressure in the inner surface of the stent produces comparable values to LE1 and hyperelastic models of required expansion pressure, being the remaining metrics significantly higher.

ACKNOWLEDGEMENTS

The authors wish to thank: Program COMPETE funding through the projects POCI-01-0145-FEDER-016779, PTDC/EMS-TEC/0702/2014, Projecto 0702 – PPCDT e comparticipado pelo Fundo Comunitário Europeu FEDER.

REFERENCES

[1] T. Roy and A. Chanda, "Computational Modeling and Analysis of Latest Commercially Available Coronary Stents During Deployment," Procedia Mater. Sci., vol. 5, pp. 2310–2319, 2014.

[2] N. Li and Y. Gu, "Parametric design analysis and shape optimization of coronary arteries stent structure," Proc. 6th World Congr. Struct. Multidiscip. Optim. Rio Jan., vol. 30, 2005.

[3] M. Azaouzi, A. Makradi, and S. Belouettar, "Numerical investigations of the structural behavior of a balloon expandable stent design using finite element method," Comput. Mater. Sci., vol. 72, pp. 54–61, May 2013.

[4] M. Imani, A. M. Goudarzi, D. D. Ganji, and A. L. Aghili, "The comprehensive finite element model for stenting: The influence of stent design on the outcome after coronary stent placement," J. Theor. Appl. Mech., vol. 51, no. 3, pp. 639–648, 2013.

[5] A. Schiavone and L. G. Zhao, "A study of balloon type, system constraint and artery constitutive model used in finite element simulation of stent deployment," Mech. Adv. Mater. Mod. Process., vol. 1, no. 1, Dec. 2015.

[6] M. De Beule, P. Mortier, S. G. Carlier, B. Verhegghe, R. Van Impe, and P. Verdonck, "Realistic finite element-based stent design: The impact of balloon folding," J. Biomech., vol. 41, no. 2, pp. 383–389, Jan. 2008.

[7] N. Eshghi, M. H. Hojjati, M. Imani, and A. M. Goudarzi, "Finite Element Analysis of Mechanical Behaviors of Coronary Stent," Procedia Eng., vol. 10, pp. 3056–3061, 2011.

[8] M. Gay, L. Zhang, and W. K. Liu, "Stent modeling using immersed finite element method," Comput. Methods Appl. Mech. Eng., vol. 195, no. 33–36, pp. 4358–4370, Jul. 2006.

[9] W.-Q. Wang, D.-K. Liang, D.-Z. Yang, and M. Qi, "Analysis of the transient expansion behavior and design optimization of coronary stents by finite element method," J. Biomech., vol. 39, no. 1, pp. 21–32, Jan. 2006.

[10] F. Gervaso, C. Capelli, L. Petrini, S. Lattanzio, L. Di Virgilio, and F. Migliavacca, "On the effects of different strategies in modeling balloon-expandable stenting by means of finite element method," J. Biomech., vol. 41, no. 6, pp. 1206–1212, 2008.

[11] S. Pant, N. W. Bressloff, and G. Limbert, "Geometry parameterization and multidisciplinary constrained optimization of coronary stents," Biomech. Model. Mechanobiol., vol. 11, no. 1–2, pp. 61–82, Jan. 2012.

[12] A. Schiavone and L. G. Zhao, "A computational study of stent performance by considering vessel anisotropy and residual stresses," Mater. Sci. Eng. C, vol. 62, pp.

307–316, May 2016.
[13] A. Schiavone, C. Abunassar, S. Hossainy, and L. G. Zhao, “Computational analysis of mechanical stress–strain interaction of a bioresorbable scaffold with blood vessel,” J. Biomech., vol. 49, no. 13, pp. 2677–2683, Sep. 2016.
[14] Z. Guo and L. J. Sluys, “Constitutive modeling of hyperelastic rubber-like materials,” HERON 53 3, 2008.
[15] S. N. David Chua, B. J. Mac Donald, and M. S. J. Hashmi, “Finite element simulation of stent and balloon interaction,” J. Mater. Process. Technol., vol. 143–144, pp. 591–597, Dec. 2003.
[16] B. Beigzadeh, S. A. Mirmohammadi, and M. R. Ayatollahi, “A numerical study on the effect of geometrical parameters and loading profile on the expansion of stent,” Biomed. Mater. Eng., vol. 28, no. 5, pp. 463–476, Aug. 2017.
[17] I. V. Gomes, H. Puga, and J. L. Alves, “Shape and functional optimization of biodegradable magnesium stents for manufacturing by ultrasonic-microcasting technique,” Int. J. Interact. Des. Manuf. IJIDeM, Dec. 2017.
[18] H. Li et al., “Design optimization of stent and its dilatation balloon using kriging surrogate model,” Biomed. Eng. OnLine, vol. 16, no. 1, Dec. 2017.
[19] H. Zahedmanesh, D. John Kelly, and C. Lally, “Simulation of a balloon expandable stent in a realistic coronary artery—Determination of the optimum modeling strategy,” J. Biomech., vol. 43, no. 11, pp. 2126–2132, Aug. 2010.